IEEE Access
Multidisciplinary : Rapid Review : Open Access Journal

Received May 24, 2020, accepted May 30, 2020, date of publication June 3, 2020, date of current version June 18, 2020.
Digital Object Identifier 10.1109/ACCESS.2020.2999623

An Analytical Method to Investigate Propagation Properties of Magnetostatic Biased Graphene Layers

YAO MA, LIHUA SHI, (Member, IEEE), JIANBAO WANG, JIE LI, YICHENG LIU, AND YUZHOU RAN
National Key Laboratory on Electromagnetic Environment Effects and Electro-Optical Engineering, Army Engineering University of PLA, Nanjing 210007, China

Corresponding author: Jianbao Wang (zwang0417@outlook.com)

This work was supported by the National Nature Science Foundation of China under Grant 51977219.

ABSTRACT The transmission and reflection properties of magnetostatic biased graphene layers are investigated based on analytical method, where graphene is treated as a bulk material. Considering the anisotropic nature of the magnetostatic biased graphene (magnetized graphene), the generalized reflection and transmission coefficients of a plane wave incidence on anisotropic multilayer structures are first derived. The accuracy of this method is validated by a numerical example of a plane wave incidence on a magnetized monolayer graphene in free space. Based on this model, the transmission coefficient decreases with increasing the incident angle for the TE (transverse electric) polarized wave incidence, while an opposite phenomenon occurs for the TM (transverse magnetic) polarized wave incidence. The transmission properties can be also modulated by changing the external static magnetic field. The electromagnetic propagation properties of composites consisting of magnetized graphene and dielectric layers are also analyzed based on this method. The transmission properties degrade with increasing the number of magnetized graphene layers.

INDEX TERMS Magnetostatic biased graphene, reflection properties, transmission properties.

I. INTRODUCTION

Graphene has attracted much attention due to its superior electrical, thermal, optical and mechanical properties [1]. Surface conductivity is a key parameter usually used for describing the electromagnetic properties of graphene. Generally, the expression of surface conductivity can be categorized into three forms [2]: (i) in the case of spatial dispersion but with neither electrostatic nor magnetostatic bias, the surface conductivity can be expressed by an operator; (ii) when graphene is biased by a static electric field with neither static magnetic field nor spatial dispersion, the surface conductivity is a scalar and the corresponding graphene can be regarded as an isotropic material; (iii) when graphene is biased by a static magnetic field and also possibly a static electric field (but with no spatial dispersion), the surface conductivity is a tensor. Particularly, in the case of (iii), graphene is an anisotropic material with gyrotropic and electromagnetic nonreciprocal properties, and thus has a great potential in applications of nonreciprocal and gyrotropic microwave/terahertz devices [3], [4].

So far, two main methods have been reported to establish the electromagnetic model for investigating the interaction between the electromagnetic field and the graphene. In one method, graphene is regarded as a two-dimensional (2-D) conductive sheet [3]–[7]; in the other method, graphene is treated as a bulk material [8]–[14]. Based on the first method with graphene as a 2-D sheet, Sounas and Caloz successfully obtained the analytic expressions of the reflection and transmission coefficients when a plane wave obliquely incidents on a magnetostatic biased graphene sheet in free space [3]. This original work has opened up a new strategy in revealing the fundamentals of gyrotropy and nonreciprocity of graphene. Therefore, it has received much attention. Recently, considering that periodic arrays of magnetically-biased graphene ribbons are one of the most popular

The associate editor coordinating the review of this manuscript and approving it for publication was Chan Hwang See.

graphene-based structures, Memarian *et al.* proposed an analytical method for the analysis of this structure. Based on integral equations governing the field and the surface current density on magnetically biased graphene ribbons, this new method is precise, reliable, and affordable [7]. It is noted that it is not easy to experimentally prepare monolayer graphene and alternatively graphene used in practice usually consists of several layers. The above facts suggest that it is more suitable for graphene to be modeled as a bulk material than a 2-D sheet under this circumstance.

On the other hand, besides the interaction between the electromagnetic field and the surface of graphene, the propagation of the electromagnetic wave inside graphene also needs to be considered when graphene is regarded as a bulk material. This significantly enhances the difficulty of analytic modeling, and thus leads to a fact that the numerical algorithms (e.g. the finite-difference time-domain (FDTD) algorithm) are mainly adopted when graphene is regarded as a bulk material [8]–[11]. However, the ultra-thin nature of the graphene would inevitably increases the numbers of grids (and thus degrading the simulation efficiency) for the conventional FDTD algorithm. To address this issue, many improved FDTD algorithms (e.g. unconditionally stable and weakly conditionally stable FDTD algorithms) have been developed, which can improve the simulation efficiency without sacrificing the simulation precision [8]–[10]. However, the numerical algorithms reported in the literatures only solved the simple problem of normal plane wave incidence on a monolayer graphene, and the problems associated with oblique plane wave incidence on multilayer graphene are rarely solved due to computational efficiency.

To the best of our knowledge, little effort has been made to provide an effective method to study the electromagnetic transmission and reflection properties of magnetized graphene layers when the graphene is modeled as a bulk material. Therefore, this paper offers the analytical formulations of the generalized transmission and reflection coefficients of a plane wave incidence on anisotropic multilayer structures based on the transfer matrix method (TMM). It is noted that, this work mainly focuses on the applications of graphene in the fields of electromagnetic shielding (EMC) and absorbers, therefore, the linearly polarized wave incidence, rather than the circularly polarized wave incidence is utilized in this work [12]–[14]. Then the electromagnetic propagation properties of both magnetized monolayer graphene and composites consisting of magnetized graphene layers and dielectrics can be analyzed.

The paper is organized as follows. Firstly, the problem of an oblique plane wave incidence on an anisotropic multilayer structure is solved to infer the generalized reflection and transmission coefficients. Secondly, a numerical example of a plane wave incidence on a magnetized monolayer graphene in free space is calculated to validate the accuracy of this modeling method by comparison with the work in the literature [3]. The influences of incident angle and external magnetic field on the propagation properties of this graphene layer are discussed. Finally, the paper provides numerical examples of oblique plane wave incidence on composites consisting of magnetized graphene layers and dielectrics, and analyzes the reflection and transmission properties of these structures.

II. FORMULATIONS

A. ELECTROMAGNETIC PARAMETERS OF THE MAGNETIZED GRAPHENE

When a graphene layer is biased with a perpendicular static magnetic field B_0, it exhibits anisotropy and its surface conductivity $\bar{\bar{\sigma}}$ is a tensor as discussed earlier and can be described by the following equation

$$\bar{\bar{\sigma}} = \begin{bmatrix} \sigma_{xx}(\omega) & \sigma_{xy}(\omega) \\ \sigma_{yx}(\omega) & \sigma_{yy}(\omega) \end{bmatrix} \tag{1}$$

In the above equation, the diagonal conductivity σ_{xx}, σ_{yy} and the off-diagonal conductivity σ_{xy}, σ_{yx} can be expressed in the Drude model form according to [3], [15]

$$\sigma_{xx}(\omega, B_0) = \sigma_{yy}(\omega, B_0) = \sigma_0 \frac{1 + j\omega\tau}{(\omega_c\tau)^2 + (1 + j\omega\tau)^2} \tag{2}$$

$$\sigma_{yx}(\omega, B_0) = -\sigma_{xy}(\omega, B_0) = \sigma_0 \frac{\omega_c\tau}{(\omega_c\tau)^2 + (1 + j\omega\tau)^2} \tag{3}$$

where

$$\sigma_0 = \frac{2e^2\tau}{\pi\hbar^2} k_B T \ln(2\cosh\frac{\mu_c}{2k_B T}) \tag{4}$$

$$\omega_c = \frac{eB_0 v_F^2}{\mu_c} \tag{5}$$

where e is the single electron charge, τ is the scattering time, h is the reduced Planck's constant, k_B is the Boltzmann constant, T is the operating temperature. μ_c is the chemical potential, ω_c is the cyclotron frequency and v_F is the Fermi velocity. Formulas (2)-(5) are valid under the conditions of $\mu_C \gg k_B T$ and $\mu_C \gg \hbar\omega$ [16], [17].

The permittivity and permeability of the magnetostatic biased graphene can be expressed by

$$\bar{\varepsilon} = \begin{bmatrix} \varepsilon_{11} & \varepsilon_{12} & 0 \\ \varepsilon_{21} & \varepsilon_{22} & 0 \\ 0 & 0 & \varepsilon_0 \end{bmatrix} \tag{6}$$

$$\bar{\mu} = \begin{bmatrix} \mu_0 & 0 & 0 \\ 0 & \mu_0 & 0 \\ 0 & 0 & \mu_0 \end{bmatrix} \tag{7}$$

where

$$\varepsilon_{11} = \varepsilon_{22} = \varepsilon_0 - i\frac{\sigma_{xx}}{\omega\Delta z} \tag{8}$$

$$\varepsilon_{21} = -\varepsilon_{12} = -i\frac{\sigma_{yx}}{\omega\Delta z} \tag{9}$$

where ε_0 is the vacuum permittivity and μ_0 is the vacuum permeability.

B. PLANE WAVE IN MAGNETIZED GRAPHENE

The time harmonic form of the Maxwell's equations in a passive, lossless and anisotropic material is described as

$$\nabla \times E = -j\omega\bar{\mu} \cdot H \tag{10}$$

$$\nabla \times H = j\omega\bar{\varepsilon} \cdot E \tag{11}$$

$$\nabla \cdot D = 0 \tag{12}$$

$$\nabla \cdot B = 0 \tag{13}$$

For an anisotropic material, the TE and TM polarized waves would couple with each other, that is, when the material is illuminated by a TE (or TM) polarized wave, both TE and TM modes exist in the reflected and transmitted waves simultaneously. Consequently, the wave equations in anisotropic materials are vector equations, which can be easily solved by using the state variable method [18]. In order to facilitate using the boundary conditions, we deduce the state equations of the transverse components of the electric and magnetic fields (suppose that the propagation direction of the plane wave is parallel to the z axis in the Cartesian coordinate system).

By decomposing the two curl equations of the Maxwell's equations into the transverse and vertical components respectively and eliminating the vertical components, we get the following state equation

$$\frac{d}{dz}V = jH \cdot V \tag{14}$$

where $V = [E_x, E_y, H_x, H_y]^{\mathrm{T}}$ is the state variable, and H is a 4×4 matrix related to the parameters of frequency, permittivity, permeability and transverse wave number. H is also called the coupling matrix, which can be described as

$$[H] = \begin{bmatrix} 0 & 0 & -\frac{k_x k_y}{\omega\varepsilon_0} & -\omega\mu_0 + \frac{k_x k_x}{\omega\varepsilon_0} \\ 0 & 0 & \omega\mu_0 - \frac{k_y k_y}{\omega\varepsilon_0} & \frac{k_x k_y}{\omega\varepsilon_0} \\ \omega\varepsilon_{21} + \frac{k_x k_y}{\omega\mu_0} & \omega\varepsilon_{11} - \frac{k_x k_x}{\omega\mu_0} & 0 & 0 \\ -\omega\varepsilon_{11} + \frac{k_y k_y}{\omega\mu_0} & \omega\varepsilon_{21} - \frac{k_x k_y}{\omega\mu_0} & 0 & 0 \end{bmatrix} \tag{15}$$

In the above equation, $k_x = k\sin\theta\cos\varphi$ and $k_y = k\sin\theta\sin\varphi$ are the transverse wave numbers, where k is the amplitude of wave vector, θ is the pitch angle and φ is the azimuth angle.

According to the boundary conditions, transverse components of electric and magnetic fields are continuous at the interface, so equation (14) is a first-order ordinary differential equation. Its general solution is

$$V = V_0 e^{j\lambda z} \tag{16}$$

inserting (16) into (14) yields

$$(H - \lambda I) \cdot V_0 = 0 \tag{17}$$

which can be ascribed to an eigenvalue problem. Since H is a 4×4 square matrix, (17) has four eigenvalues and four eigenvectors. So the general solution described by (16) has the following form

$$V(z) = A_1 a_1 e^{j\beta_1 z} + A_2 a_2 e^{j\beta_2 z} + A_3 a_3 e^{-j\beta_3 z} + A_4 a_4 e^{-j\beta_4 z} \tag{18}$$

where A_i is amplitude, β_i is eigenvalue and a_i is the eigenvector for the eigenvalue β_i. The four components represent the TE and TM polarized wave propagating along the z and -z directions respectively.

Suppose an infinite magnetized graphene layer with its two surfaces perpendicular to the z axis, when a plane wave obliquely incident on the graphene in the xoz plane, the coupling matrix H becomes

$$[H] = \begin{bmatrix} 0 & 0 & 0 & -\omega\mu_0 + \frac{k_x k_x}{\omega\varepsilon_0} \\ 0 & 0 & \omega\mu_0 & 0 \\ \omega\varepsilon_{21} & \omega\varepsilon_{11} - \frac{k_x k_x}{\omega\mu_0} & 0 & 0 \\ -\omega\varepsilon_{11} & \omega\varepsilon_{21} & 0 & 0 \end{bmatrix} \tag{19}$$

By substituting (19) into (17), the eigenvalues and eigenvectors are

$$\begin{aligned} \beta_1 &= \sqrt{\frac{m_1 + m_2}{2\varepsilon_0}}, \quad \beta_2 = \sqrt{\frac{m_1 - m_2}{2\varepsilon_0}} \\ \beta_3 &= -\sqrt{\frac{m_1 + m_2}{2\varepsilon_0}}, \quad \beta_4 = -\sqrt{\frac{m_1 - m_2}{2\varepsilon_0}} \end{aligned} \tag{20}$$

$$a_1 = \begin{bmatrix} \frac{\beta_1(\varepsilon_0\beta_1^2 + m_2)}{\varepsilon_0 m_3} \\ \frac{\beta_1(\varepsilon_0\varepsilon_{11}\beta_1^2 + m_4)}{\varepsilon_0\varepsilon_{21} m_3} \\ m_5 - \frac{m_1 + m_2}{2\mu_0\varepsilon_0\varepsilon_{21}\omega^2} \\ 1 \end{bmatrix}, \quad a_2 = \begin{bmatrix} \frac{\beta_2(\varepsilon_0\beta_2^2 + m_2)}{\varepsilon_0 m_3} \\ \frac{\beta_2(\varepsilon_0\varepsilon_{11}\beta_2^2 + m_4)}{\varepsilon_0\varepsilon_{21} m_3} \\ m_5 + \frac{m_1 - m_2}{2\mu_0\varepsilon_0\varepsilon_{21}\omega^2} \\ 1 \end{bmatrix}$$

$$a_3 = \begin{bmatrix} -\frac{\beta_1(\varepsilon_0\beta_1^2 + m_2)}{\varepsilon_0 m_3} \\ -\frac{\beta_1(\varepsilon_0\varepsilon_{11}\beta_1^2 + m_4)}{\varepsilon_0\varepsilon_{21} m_3} \\ m_5 - \frac{m_1 + m_2}{2\mu_0\varepsilon_0\varepsilon_{21}\omega^2} \\ 1 \end{bmatrix}, \quad a_4 = \begin{bmatrix} -\frac{\beta_2(\varepsilon_0\beta_2^2 + m_2)}{\varepsilon_0 m_3} \\ -\frac{\beta_2(\varepsilon_0\varepsilon_{11}\beta_2^2 + m_4)}{\varepsilon_0\varepsilon_{21} m_3} \\ m_5 + \frac{m_1 - m_2}{2\mu_0\varepsilon_0\varepsilon_{21}\omega^2} \\ 1 \end{bmatrix} \tag{21}$$

where

$$\begin{aligned} m_1 &= -\sqrt{k_x^4(\varepsilon_0 - \varepsilon_{11})^2 + 4\mu_0\varepsilon_0\varepsilon_{21}^2\omega^2(k_x^2 - \mu_0\varepsilon_0\omega^2)} \\ m_2 &= k_x^2(\varepsilon_0 + \varepsilon_{11}) - 2\mu_0\varepsilon_0\varepsilon_{11}\omega^2 \\ m_3 &= \omega(\mu_0\varepsilon_{11}^2\omega^2 - k_x^2\varepsilon_{11} + \mu_0\varepsilon_{21}^2\omega^2) \\ m_4 &= k_x^2\varepsilon_{11}^2 + \mu_0\varepsilon_0\omega^2(\varepsilon_{21}^2 - \varepsilon_{11}^2) \\ m_5 &= (k_x^2\varepsilon_{11} - \mu_0\varepsilon_0\varepsilon_{11}\omega^2)/(\mu_0\varepsilon_0\varepsilon_{21}\omega^2) \end{aligned} \tag{22}$$

By substituting the eigenvalues and eigenvectors into (18), the electromagnetic field in magnetized graphene can be

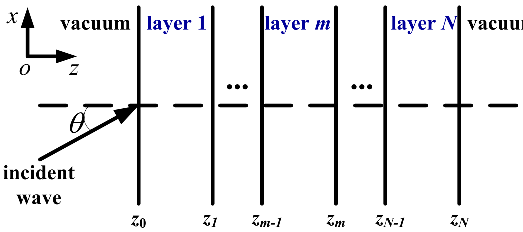

FIGURE 1. Plane wave incidence on an anisotropic multilayer structure.

obtained in the matrix form

$$V(z) = \bar{a} \cdot e^{j\bar{\beta} z} \cdot \bar{A} \tag{23}$$

where $\bar{a} = [a_1 \quad a_2 \quad a_3 \quad a_4]$, $\bar{A} = [A_1 \quad A_2 \quad A_3 \quad A_4]^{\mathrm{T}}$, and

$$e^{j\bar{\beta} z} = \begin{bmatrix} e^{j\beta_1 z} & 0 & 0 & 0 \\ 0 & e^{j\beta_2 z} & 0 & 0 \\ 0 & 0 & e^{-j\beta_3 z} & 0 \\ 0 & 0 & 0 & e^{-j\beta_4 z} \end{bmatrix} \tag{24}$$

This arrangement means that the first two diagonal elements represent electromagnetic wave propagating along the -z direction, while the latter two diagonal elements represent electromagnetic wave propagating along the z direction.

III. REFLECTION AND TRANSMISSION PROPERTIES OF ANISOTROPIC MULTILAYER STRUCTURES

Regarding a multilayer structure with N layers of anisotropic materials in Fig.1, the generalized reflection coefficient (the ratio of the reflected field with the incident field) and transmission coefficient (the ratio of the transmitted field with the incident field) can be solved by using the transfer matrix method [18].

A. THE GENERALIZED REFLECTION COEFFICIENT

For the vacuum adjacent to the left side of the 1*st* layer (denoted as layer 1) in Fig.1, the state variable of electromagnetic field is

$$V_0(z) = \bar{a}_0 \cdot e^{j\bar{\beta}_0 z} \cdot \bar{A}_0 \tag{25}$$

The relationship between the electromagnetic fields in the vacuum and the 1st layer material at the interface $z = z_0$ can be expresses as

$$\begin{bmatrix} A_{10} e^{j\beta_{10} z_0} \\ A_{20} e^{j\beta_{20} z_0} \end{bmatrix} = [R_{01}] \begin{bmatrix} A_{30} e^{-j\beta_{10} z_0} \\ A_{40} e^{-j\beta_{20} z_0} \end{bmatrix} \tag{26}$$

where R_{01} is the generalized reflection coefficient matrix at the interface $z = z_0$. For reflection wave of the TE and TM modes propagating along the -z direction, A_{10} and A_{20} represent their amplitude respectively, while A_{30} and A_{40} represent amplitude of the TE and TM polarized transmitted waves propagating along the z direction.

Assume that A_{30} and A_{40} are known and A_{10} and A_{20} or R_{01} are unknowns, then the state variable at $z = z_0$ can be written as

$$V_0(z_0) = \bar{a}_0 \cdot \begin{bmatrix} R_{01} \\ I \end{bmatrix} \begin{bmatrix} A_{30} e^{-j\beta_{10} z_0} \\ A_{40} e^{-j\beta_{20} z_0} \end{bmatrix} \tag{27}$$

B. THE GENERALIZED TRANSMISSION COEFFICIENT

For the vacuum adjacent to the right side of the Nth layer in Fig. 1, the state variable of the electromagnetic field is

$$V_{N+1}(z) = \bar{a}_{N+1} \cdot e^{j\bar{\beta}_{N+1} z} \cdot \bar{A}_{N+1} \tag{28}$$

The relationship between the electromagnetic fields in the Nth layer material and the vacuum at the interface $z = z_N$ can be expresses as

$$\begin{bmatrix} A_{3(N+1)} e^{-j\beta_{1(N+1)} z_N} \\ A_{4(N+1)} e^{-j\beta_{2(N+1)} z_N} \end{bmatrix} = [T_{0N}] \begin{bmatrix} A_{30} e^{-j\beta_{10} z_0} \\ A_{40} e^{-j\beta_{20} z_0} \end{bmatrix} \tag{29}$$

where T_{0N} is the generalized transmission coefficient matrix. For transmitted wave of the TE and TM modes propagating along the z direction, $A_{3(N+1)}$ and $A_{4(N+1)}$ represent their amplitude respectively.

Considering that there is no reflection wave along the -z direction in the vacuum, the state variable at $z = z_N$ can be written as

$$V_{N+1}(z_N) = \bar{a}_{N+1} \cdot \begin{bmatrix} 0 \\ T_{0N} \end{bmatrix} \begin{bmatrix} A_{30} e^{-j\beta_{10} z_0} \\ A_{40} e^{-j\beta_{20} z_0} \end{bmatrix} \tag{30}$$

C. THE TRANSFER MATRIX FROM $z = z_0$ TO $z = z_N$

The state variable of (23) in layer m can be rewritten as

$$\begin{aligned} V_m(z) &= \bar{a}_m \cdot e^{j\bar{\beta}_m z} \cdot \bar{A}_m \\ &= \bar{a}_m \cdot e^{j\bar{\beta}_m (z-z')} \cdot \bar{a}_m^{-1} \cdot \bar{a}_m \cdot e^{j\bar{\beta}_m z'} \cdot \bar{A}_m \\ &= \bar{a}_m \cdot e^{j\bar{\beta}_m (z-z')} \cdot \bar{a}_m^{-1} \cdot V_m(z') \\ &= \bar{P}_m(z, z') \cdot V_m(z') \end{aligned} \tag{31}$$

where $\bar{P}_m(z, z') = \bar{a}_m \cdot e^{j\bar{\beta}_m (z-z')} \cdot \bar{a}_m^{-1}$ is the transfer matrix from z to z' in layer m.

For layer m, the electromagnetic field at interfaces $z = z_{m-1}$ and $z = z_m$ can be linked through

$$V_m(z_m) = \bar{P}(z_m, z_{m-1}) \cdot V_m(z_{m-1}) \tag{32}$$

According to the boundary conditions that transverse components of the electromagnetic field are continuous at the interface, the following equation can be obtained

$$V_m(z_{m-1}) = V_{m-1}(z_{m-1}) \tag{33}$$

thus,

$$\begin{aligned} V_{N+1}(z_N) = V_N(z_N) &= \bar{P}_N(z_N, z_{N-1}) \cdot V_N(z_{N-1}) \\ &= \bar{P}_N(z_N, z_{N-1}) \cdots \bar{P}_1(z_1, z_0) \cdot V_0(z_0) \\ &= \bar{P}(z_N, z_0) \cdot V_0(z_0) \end{aligned} \tag{34}$$

where $\bar{P}(z_N, z_0) = \prod_{m=N}^{1} \bar{P}_m(z_m, z_{m-1})$ is the transfer matrix from $z = z_0$ to $z = z_N$.

Substituting (27) and (30) into (34) yeilds

$$\begin{bmatrix} 0 \\ T_{0N} \end{bmatrix} = \bar{a}_{N+1}^{-1} \cdot \bar{P}(z_N, z_0) \cdot \bar{a}_0 \cdot \begin{bmatrix} R_{01} \\ I \end{bmatrix} \tag{35}$$

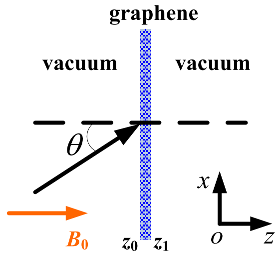

FIGURE 2. A schematic of a plane wave incidence on a magnetized monolayer graphene in free space.

define

$$[G]=\bar{a}_{N+1}^{-1}\cdot\bar{P}\left(z_N,z_0\right)\cdot\bar{a}_0=\begin{bmatrix} g_1 & g_2 \\ g_3 & g_4\end{bmatrix} \tag{36}$$

where $[g_1]$-$[g_4]$ are 2×2 matrixes.

Finally, the generalized reflection and transmission coefficients can be obatined

$$[R_{01}]=-[g_1]^{-1}[g_2] \tag{37}$$

$$[T_{0N}]=[g_3][R_{01}]+[g_4] \tag{38}$$

IV. NUMERICAL EXAMPLES

A. TRANSMISSION PROPERTIES OF A MAGNETIZED MONOLAYER GRAPHENE

Fig. 2 shows the schematic of an infinite monolayer graphene in free space with its two surfaces perpendicular to the z axis. The graphene is biased by a static magnetic field B_0 which is along the z-axis direction. A plane wave incident on the graphene in the xoz plane with an incident angle θ.

In this case, the transfer matrix of the graphene layer can be written as

$$\bar{P}_1\left(z_1,z_0\right)=\bar{a}_1\cdot e^{j\bar{\beta}_1(z_1-z_0)}\cdot\bar{a}_1^{-1} \tag{39}$$

where $z_1-z_0=0.34nm$ is the thickness of a single graphene layer [19]–[21].

When $T=300K$, $\mu_c=0.117eV$ and $B_0=2T$, we first calculate the transmission coefficient of the magnetized graphene layer with different incident angles for both TE and TM polarized wave incidences. To validate the accuracy of our method, we also calculate the transmission coefficient by using the following formulation [3]:

$$\bar{\bar{T}}_{21}=2\frac{\begin{bmatrix} 2+Z^h\sigma_{xx} & Z^e\sigma_{yx} \\ -Z^h\sigma_{yx} & 2+Z^e\sigma_{xx}\end{bmatrix}}{(2+Z^e\sigma_{xx})(2+Z^h\sigma_{xx})+(\eta_0\sigma_{yx})^2} \tag{40}$$

where $\eta_0=\sqrt{\mu_0/\varepsilon_0}$ is the wave impedance of free space, $Z^e=k_z/(\omega\varepsilon_0)$ and $Z^h=\omega\mu_0/k_z$ are the wave impedance of the E(TM) and H(TE) polarized waves respectively. Comparison between these two results is shown in Fig. 3.

Graphene is modeled as a 2-D conductive sheet in [3], while it is treated as a bulk material in our work. The following conclusions can be obtained according to Fig. 3: (1) firstly, the results in our work coincide well with those reported in [3] for both normal incidence and oblique incidence, thus validating the accuracy of our method. (2) Secondly, when the plane wave is normally incident, the transmission coefficient is equal for both TE and TM wave incidence, and thus the four curves (denoted as TE_0°_ref [3], TE_0°_our, TM_0°_ref [3], TM_0°_our) overlap. (3) Thirdly, for the TE polarized wave incidence, the transmission property decreases with increasing the incident angle θ, while for the TM polarized wave incidence, it shows an opposite phenomenon. This could be explained as following. For the TE polarized wave, the electric field is always parallel to the graphene surface for all incident angles, and so graphene always interacts with the wave. As θ increases, the interaction between the incident wave and graphene enhances and thus leading to the transmission decreases. For the TM polarized wave, the component of the electric field parallel to the graphene surface decreases with increasing the incident angle θ, and the field becomes completely perpendicular to the graphene surface as θ is 90°. Therefore, the interaction between the incident wave and the graphene attenuates with increasing the incident angle θ, thus leading to the transmission increases. In addition, all the transmission spectra displays minimum points. This should be due to that the worst impedance matching between the graphene characteristic impedance and the air characteristic impedance occurs at this frequency.

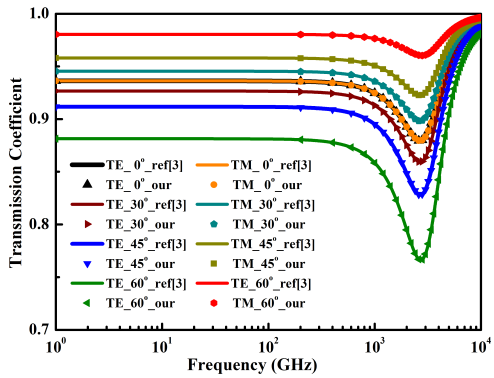

FIGURE 3. Transmission coefficient of a magnetized monolayer graphene under the TE and TM polarized waves incidence for different incident angles in free space.

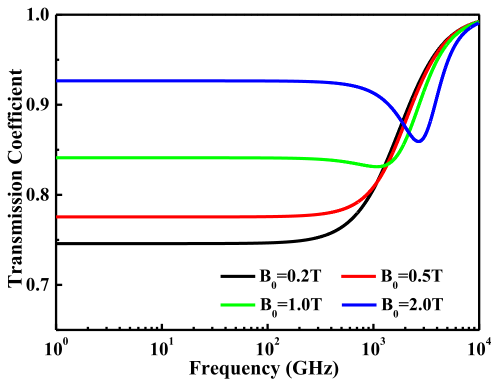

FIGURE 4. Transmission coefficient of a monolayer graphene biased by different static magnetic fields B_0 for the TE polarized wave incidence.

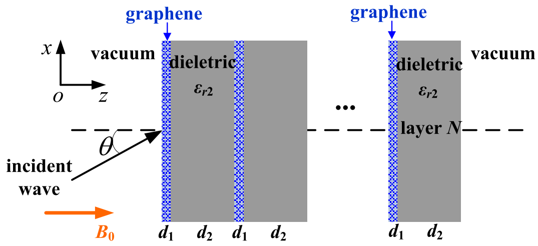

FIGURE 5. A schematic of a plane wave incidence on a multilayer structure of alternate graphene and dielectric layers in free space.

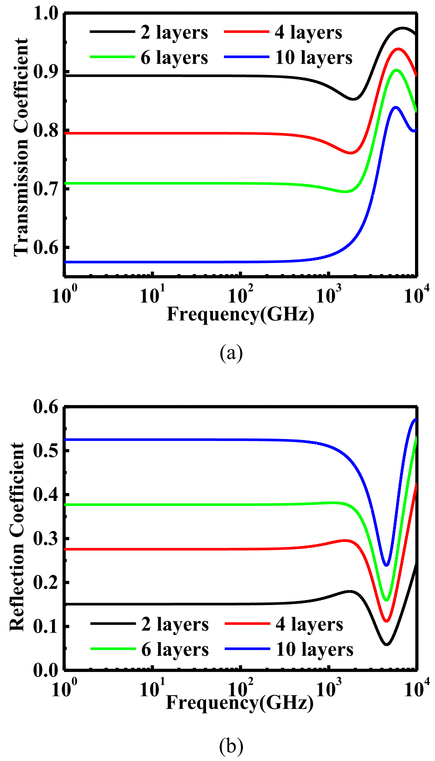

FIGURE 6. The transmission and reflection coefficients of the multilayer structure with different N for the TE polarized wave incidence (a) the transmission coefficient (b) the reflection coefficient.

The transmission coefficient is also influenced by the external static magnetic field B_0, as shown in Fig. 4. When B_0 increases from $0.2T$ to $2.0T$, the transmission coefficient increases obviously for the TE polarized wave incidence. For the TM polarized wave incidence, its transmission coefficient also increases with increasing B_0.

B. PROPAGATION PROPERTIES OF MULTILAYER STRUCTURES CONTAINING MAGNETIZED GRAPHENE LAYERS

Since the graphene/dielectric composites are widely used in applications, a typical multilayer structure of this composite is shown in Fig. 5, which consisting of alternate graphene and dielectric layers. The thicknesses of each graphene and dielectric layers are d_1 and d_2 respectively, and the relative dielectric constant of the dielectric layer is ε_{r2}.

The transmission and reflection coefficients of this multilayer structure with different number of layers (denoted as N)

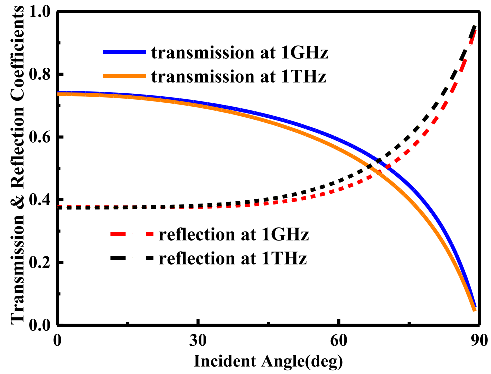

FIGURE 7. The transmission and reflection coefficients of the multilayer structure when N = 6 versus incident angle for the TE polarized wave incidence.

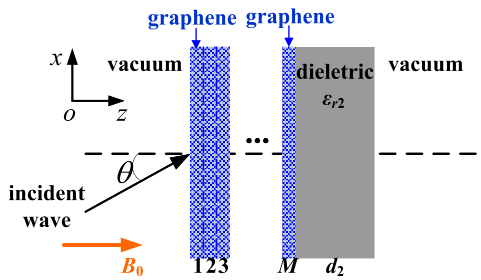

FIGURE 8. A schematic of a plane wave incidence on the M + 1 structure in free space.

under the TE polarized wave incidence are shown in Fig. 6. Here, B_0 is $2T$, ε_{r2} is 2.25 [13], d_2 is 1μm, and the incident angle θ is $\pi/6$. From the result it can be concluded that the transmission properties degrade while the reflection properties improve with increasing the number of magnetized graphene layers.

When the number of layers is N = 6, the transmission and reflection coefficients versus different incidence angles at 1GHz and 1THz are shown in Fig. 7. It can be found that for the TE polarized wave incidence, the transmission decreases while the reflection increases when the incident angle θ increases, the reason is the same as that of TE and TM waves incidence on a monolayer graphene as mentioned before.

As it mentioned earlier, the graphene in practice is usually consisted of several layers due to the preparation constraint. For instance, the graphene prepared by the supercritical fluid stripping method is about 5 layers. So another composite structure (called the $M + 1$ structure below) is shown in Fig. 8. This structure is consisted of M continuous layers of magnetized graphene and one single layer of dielectric whose relative dielectric constant is ε_{r2} and thickness is d_2.

Fig. 9 shows the transmission coefficient and reflection coefficient of this structure for the TE polarized wave incidence with an incident angle $\theta = \pi/6$ when M takes different numbers. The chemical potential μ_c of the $M + 1$ structure is assumed to be the same as that of the monolayer graphene structure. It can be found that when M increases from 1 to 5, the transmission coefficient declines obviously while the reflection coefficient takes a remarkable increase.

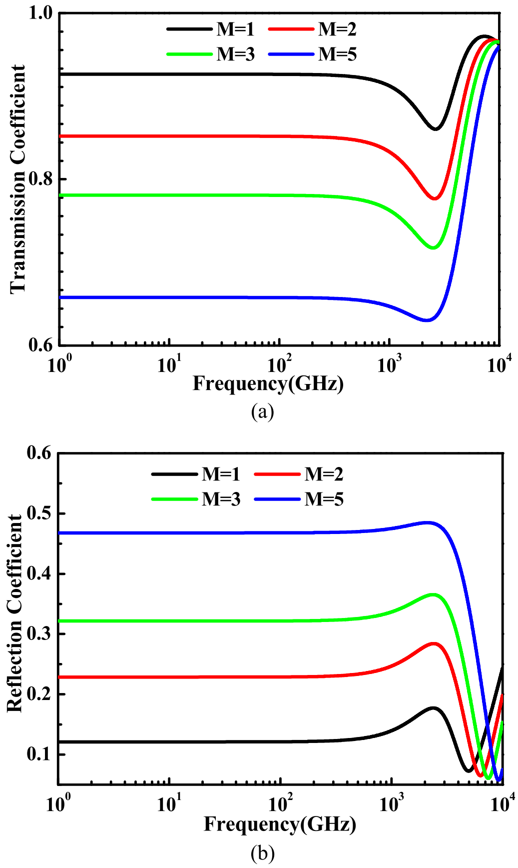

FIGURE 9. The transmission and reflection coefficients of the M + 1 structure with different M for the TE polarized wave incidence (a) the transmission coefficient (b) the reflection coefficient.

V. CONCLUSION

The transmission and reflection properties of magnetized graphene layers with graphene treated as a bulk material are studied. The accuracy of the proposed analytical method is validated by the numerical example. The method can be also used to analyze electromagnetic propagation properties of structures containing other anisotropic materials thus has a great potential for applications.

REFERENCES

[1] A. K. Geim, "Graphene: Status and prospects," *Science*, vol. 324, no. 5934, pp. 1530–1534, Jun. 2009.
[2] G. W. Hanson, "Dyadic Green's functions for an anisotropic, non-local model of biased graphene," *IEEE Trans. Antennas Propag.*, vol. 56, no. 3, pp. 747–757, Mar. 2008.
[3] D. L. Sounas and C. Caloz, "Gyrotropy and nonreciprocity of graphene for microwave applications," *IEEE Trans. Microw. Theory Techn.*, vol. 60, no. 4, pp. 901–914, Apr. 2012.
[4] I. Crassee, J. Levallois, A. L. Walter, M. Ostler, A. Bostwick, E. Rotenberg, T. Seyller, D. van der Marel, and A. B. Kuzmenko, "Giant Faraday rotation in single- and multilayer graphene," *Nature Phys.*, vol. 7, no. 1, pp. 48–51, Jan. 2011.
[5] A. G. Ardakani, Z. Ghasemi, and M. M. Golshan, "A new transfer matrix for investigation of surface plasmon modes in multilayer structures containing anisotropic graphene layers," *Eur. Phys. J. Plus*, vol. 132, no. 5, p. 206, May 2017.
[6] L. G. C. Melo, "Theory of magnetically controlled low-terahertz surface plasmon-polariton modes in graphene-dielectric structures," *J. Opt. Soc. Amer. B, Opt. Phys.*, vol. 32, no. 12, pp. 2467–2477,Dec. 2015.
[7] M. Rahmanzadeh, B. Rejaei, M. Memarian, and A. Khavasi, "Analytical and rigorous method for analysis of an array of magnetically-biased graphene ribbons," *Opt. Express*, vol. 27, no. 20, pp. 28395–28409, 2019.
[8] J. Chen, J. Li, and Q. H. Liu, "Designing graphene-based absorber by using HIE-FDTD method," *IEEE Trans. Antennas Propag.*, vol. 65, no. 4, pp. 1896–1902, Apr. 2017.
[9] S. A. Amanatiadis, N. V. Kantartzis, T. Ohtani, and Y. Kanai, "Precise modeling of magnetically biased graphene through a recursive convolutional FDTD method," *IEEE Trans. Magn.*, vol. 54, no. 3, pp. 1–4, Mar. 2018.
[10] X.-H. Wang, J.-Y. Gao, and F. L. Teixeira, "Unconditionally stable LOD-FDTD for modeling transmission properties of magnetized graphene sheet," *Opt. Commun.*, vol. 442, pp. 90–94, Jul. 2019.
[11] M. Feizi, V. Nayyeri, and O. M. Ramahi, "Modeling magnetized graphene in the finite-difference time-domain method using an anisotropic surface boundary condition," *IEEE Trans. Antennas Propag.*, vol. 66, no. 1, pp. 233–241, Jan. 2018.
[12] X. Lin, Z. Wang, F. Gao, B. Zhang, and H. Chen, "Atomically thin nonreciprocal optical isolation," *Sci. Rep.*, vol. 4, no. 1, May 2015, Art. no. 4190.
[13] M. Karimi Habil and S. Roshan Entezar, "Polarization conversion and phase modulation of terahertz electromagnetic waves via graphene-dielectric structure," *Phys. Scripta*, vol. 95, no. 1, Jan. 2020, Art. no. 015503.
[14] S. Roshan Entezar and M. Karimi Habil, "Nonreciprocal optical isolation via graphene based photonic crystals," *J. Magn. Magn. Mater.*, vol. 449, pp. 33–39, Mar. 2018.
[15] V. P. Gusynin, S. G. Sharapov, and J. P. Carbotte, "On the universal AC optical background in graphene," *New J. Phys.*, vol. 11, no. 9, Sep. 2009, Art. no. 095013.
[16] L. A. Falkovsky and S. S. Pershoguba, "Optical far-infrared properties of a graphene monolayer and multilayer," *Phys. Rev. B, Condens. Matter*, vol. 76, no. 15, Oct. 2007.
[17] L. A. Falkovsky, "Optical properties of graphene," *J. Phys., Conf. Ser.* vol. 129, May 2008, Art. no. 012004.
[18] W. C. Chew, *Waves and Fields in Inhomogeneous Media*. New York, NY, USA: Van Nostrand Reinhold, 1990.
[19] C. J. Shearer, A. D. Slattery, A. J. Stapleton, J. G. Shapter, and C. T. Gibson, "Accurate thickness measurement of graphene," *Nanotechnology*, vol. 27, no. 12, Mar. 2016, Art. no. 125704.
[20] O. Ochedowski, G. Begall, N. Scheuschner, M. El Kharrazi, J. Maultzsch, and M. Schleberger, "Graphene on Si (111) 7 × 7," *Nanotechnol.*, vol. 23, Oct. 2012, Art. no. 405708.
[21] P. Nemes-Incze, Z. Osváth, K. Kamarás, and L. P. Biró, "Anomalies in thickness measurements of graphene and few layer graphite crystals by tapping mode atomic force microscopy," *Carbon*, vol. 46, no. 11, pp. 1435–1442, Sep. 2008.

YAO MA was born in Jiangsu, China, in 1984. She received the B.S. degree in electronics information engineering from Suzhou Science and Technology University, Suzhou, China, in 2006, and the M.S. degree in electromagnetic field and microwave technology from Southeast University, Nanjing, China, in 2009. She is currently pursuing the Ph.D. degree in armament science and technology with the Army Engineering University of PLA, Nanjing.

Her research interests include computational electromagnetics and metamaterials.

LIHUA SHI (Member, IEEE) received the B.S. degree in electronic engineering from Xidian University, Xi'an, China, in 1990, the M.S. degree in electrical engineering from the Nanjing Engineering Institute, Nanjing, China, in 1993, and the Ph.D. degree in instrument science from the Nanjing University of Aeronautics and Astronautics, Nanjing, in 1996.

In 2001, he was a Visiting Scholar with Stanford University. He is currently a Professor with the National Key Laboratory on Electromagnetic Environmental Effects and Electro-Optical Engineering, Army Engineering University of PLA, Nanjing. His current research interest includes time-domain measurement technology.

Dr. Shi is a member of IEEE's Instrumentation and Measurement Society and the Electromagnetic Compatibility Society. He was a recipient of three awards from the Ministry of Science and Technology of China.

JIANBAO WANG was born in Shandong, China, in 1983. He received the B.S. degree in mechanical engineering and automation and the Ph.D. degree in armament science and technology from the PLA University of Science and Technology, Nanjing, China, in 2005 and 2014, respectively.

He is currently an Associate Professor with the National Key Laboratory on Electromagnetic Environmental Effects and Electro-Optical Engineering, Army Engineering University of PLA, Nanjing. His research interest includes computational electromagnetics.

JIE LI was born in Hunan, China, in 1996. He received the B.S. degree in camouflage engineering from the Army Engineering University of PLA, Nanjing, China, in 2018, where he is currently pursuing the Ph.D. degree with the National Key Laboratory on Electromagnetic Environmental Effects and Electro-Optical Engineering.

His current research interest includes computational electromagnetics.

YICHENG LIU was born in Yunnan, China, in 1995. He received the B.S. degree in electronics and information science and technology from Sichuan University, Chengdu, China, in 2017, and the M.S. degree in electronic science and technology from the Army Engineering University of PLA, Nanjing, China, in 2019.

His current research interest includes computational electromagnetics.

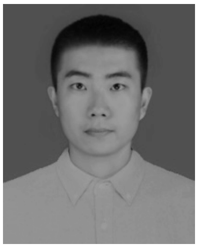

YUZHOU RAN was born in China, in 1994. He received the B.S. degree in electronic science and technology from Chongqing University, Chongqing, China, in 2016, and the M.S. degree in electromagnetic field and microwave technology from Air Force Engineering University, Xi'an, China, in 2018. He is currently pursuing the Ph.D. degree in armament science and technology with the Army Engineering University of PLA, Nanjing, China.

His current research interests include metamaterials, metasurfaces, and their applications to multifunctional devices.